

Single-electron tunneling force spectroscopy of an individual electronic state in a nonconducting surface

E. Bussmann and C. C. Williams^{a1}

Department of Physics, University of Utah, 115 South 1400 East Room 201, Salt Lake City, Utah 84112

(Received 1 March 2006; accepted 9 May 2006; published online 28 June 2006)

A tunneling spectroscopy technique to measure the energy level of an electronic state in a *completely nonconducting* surface is demonstrated. Spectroscopy is performed by electrostatic force detection of single-electron tunneling between a scanning probe and the state as a function of an applied voltage. An electronic state near the surface of a SiO₂ film is found 5.5±0.2 eV below the conduction band edge. A random telegraph signal, caused by sporadic back-and-forth single-electron tunneling, is observed as the probe Fermi level passes through the state energy. © 2006 American Institute of Physics. [DOI: 10.1063/1.2209886]

The scanning tunneling microscope (STM) provides unprecedented atomic-scale access to the electronic properties of materials.^{1–5} However, the STM requires a tunneling current, typically >0.1 pA (~10⁶ e/s), to perform measurements.⁶ Therefore, the STM cannot directly image or perform spectroscopy on any electron state with a lifetime >10⁻⁶ s—the state cannot empty fast enough to supply sufficient current. Due to the necessity for a finite tunneling current, the STM cannot be applied to nonconducting surfaces. This letter elucidates an approach to scanning tunneling spectroscopy by electrostatic force detection of tunneling of a single electron between a scanning probe and individual localized electronic states in a completely nonconducting surface.^{7–10} Spectroscopy is implemented by ramping an applied dc voltage to shift the probe Fermi level with respect to the energy of near-surface states. A random telegraph signal is observed as the probe Fermi level passes through the energy of the state. The energy level of the state is computed from the voltage at which the single-electron tunneling occurs.

Recently, single-electron tunneling measurements by force detection have been demonstrated in several types of systems. Force-detected single-electron tunneling to electronic states in nonconducting surfaces was first demonstrated by Klein and Williams using an electrostatic force microscope (EFM) in amplitude mode.^{7,8} Frequency detection EFM was used to detect and then manipulate single electrons to and from states near an insulating surface.^{9,10} Other researchers have employed force detection to observe single-electron tunneling *between* states *within* a conducting sample and to perform spectroscopic measurements.^{11–14} Single-electron charging of a localized state through which flows an average tunneling current from a scanning probe tip to a conducting substrate has also been demonstrated by electrostatic force detection.^{15,16} The work reported here demonstrates spectroscopic measurements (energy determination) of localized electronic states in a completely *nonconducting surface* by force-detected single-electron tunneling. The results demonstrate that the probe itself may serve as the electron source/sink in single-electron tunneling spectroscopic measurements. Under such conditions, spectroscopic measurements may be performed with atomic spatial resolu-

tion, as in scanning tunneling spectroscopy, but performed with single electrons.¹ This approach provides a broadly applicable technique for spectroscopic measurement of states in completely nonconducting samples, not accessible to the STM.

The basic elements of the apparatus, in a 10⁻⁸ Torr vacuum chamber at room temperature, are shown in Fig. 1(a). Single-electron tunneling events are detected between a metallic probe¹⁷ and localized electronic states near the surface of 10- and 20-nm-thick silicon dioxide (SiO₂) films on silicon substrates. The thermally grown SiO₂ films used in these experiments are known to contain bulk impurity and

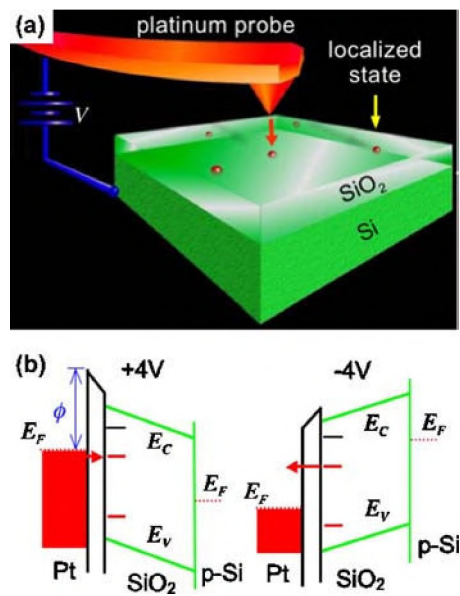


FIG. 1. (Color online) The experimental apparatus and the energy diagram for single-electron tunneling between a platinum (Pt) probe and a SiO₂ surface. (a) The basic elements of our apparatus for single-electron tunneling detection. (b) The band alignment between the Pt probe and the SiO₂ film under typical conditions for a tunneling measurement. This model treats the 10-nm-thick SiO₂ film ($\epsilon=3.9$) on a lightly doped ($10^{15}/\text{cm}^3$) *p*-type Si substrate. The band gap of SiO₂ is ~9 eV. Here $\phi=5.6$ eV is the work function of Pt. The vacuum gap z is 2 nm. Voltages of ± 4 V dc with respect to the flatband condition, typical in our measurements, allow tunneling to states within a few eV above and below the middle of the band gap. A red dash indicates a state occupied by an electron and a black dash indicates an unoccupied state. Red arrows indicate the direction of the single-electron tunneling, established by the probe Fermi level relative to the state.

^{a1}Electronic mail: clayton@physics.utah.edu

defect related localized electronic states distributed at various energies in the band gap.¹⁸ During measurements, the probe oscillates normal to the sample surface at its natural resonance frequency (~ 300 kHz) and a fixed amplitude (20–40 nm), driven by an external amplitude/frequency regulating circuit. During the oscillation cycle, the probe approaches the sample surface to a minimum vacuum gap z which is controlled on a subangstrom scale. A dc voltage V is applied to the Si substrate with respect to the grounded probe. The SiO₂ surface is prepared to eliminate adsorbed surface contamination by chemical cleaning and heating to 500–600 °C for 30 min in 10^{-8} Torr vacuum.^{7–10,19}

In these measurements, single-electron tunneling is detected by frequency detection EFM. Frequency detection EFM detects a change in the electrostatic force gradient acting on the probe apex as a shift in the resonance frequency of the oscillating force probe. Under the conditions of these measurements, the resonance frequency shift Δf is directly proportional to the electrostatic force gradient F' .⁹ A single-electron tunneling event changes the net surface charge, causing an abrupt quantized step in Δf . The charge sensitivity is limited to $\sim 0.04 e/\text{Hz}^{1/2}$ by charge fluctuation in the SiO₂. Since the 3 dB bandwidth of a typical measurement is 10 Hz, the electron must remain localized under the probe apex (nominal radius ~ 40 nm) for a time >0.015 s to be detected. Electrons that hop or tunnel quickly away from the electronic state at the surface cannot be observed. Thus, this method is complementary to the STM, in that the STM can only make direct measurements on states with short lifetimes ($<10^{-6}$ s), while this approach works only on states with long lifetimes (>0.015 s).

Direct single-electron tunneling through a vacuum gap provides unique capabilities. Since the tunneling probability is a strong function of z , varying by almost an order of magnitude per angstrom, an electron may be deposited with nanometer, or possibly subnanometer precision, as with the STM.¹ In addition, by adjusting V to tune the probe Fermi level E_F with respect to the energy of a near-surface state, an electron can be manipulated between probe and state.¹⁰ Figure 1(b) shows an energy diagram of the system consisting of the platinum metal probe and the 10-nm-thick SiO₂ on a p -type Si substrate under typical measurement conditions. The band bending is calculated using a simple one-dimensional (1D) electrostatic model and published values of the relevant physical parameters.¹⁸ The model suggests that these tunneling measurements can access states within a few eV above or below the middle of the SiO₂ band gap. The time scale to establish electronic thermal equilibrium at room temperature in SiO₂ is long compared to the time scale of our measurements, due to its large band gap (~ 9 eV).¹⁸ In addition, a 10-nm-thick SiO₂ film is sufficiently thick that the tunneling rate between the Si substrate and near-surface electronic states is negligible.²⁰ Therefore, when the probe is within tunneling range of the SiO₂, the occupation of near-surface states is largely determined by tunneling to or from the probe. When E_F is higher than an unfilled state in the surface, an electron will tunnel from the probe to the insulator. Whereas, when E_F is lower than a filled state, an electron will tunnel from the insulator to the probe. By careful measurement of the voltage at which tunneling occurs, to and from the state, its energy level can be calculated.

Frequency detection single-electron tunneling force spectroscopy is performed by fixing the probe-sample gap

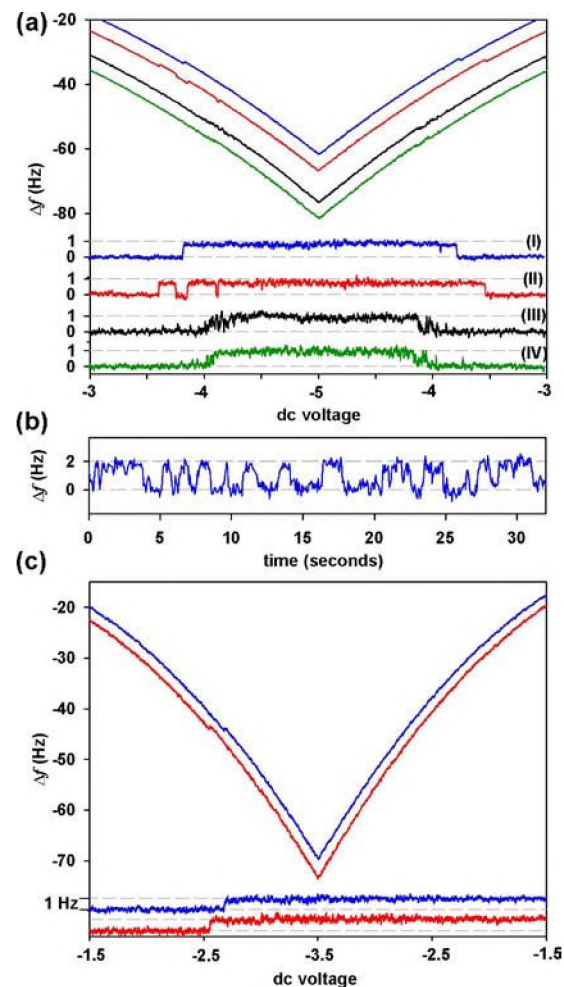


FIG. 2. (Color online) Single-electron tunneling spectroscopy of SiO₂. (a) Four consecutive measurements acquired at one location near a 10-nm-thick SiO₂ film. The tunneling event steps are shown at the bottom of Fig. 2(a) with the smooth background subtracted by a least-square fit. The state in the sample is occupied for $\Delta f=0$ Hz and unoccupied for $\Delta f=0.8$ Hz. Curves (I) and (II) were acquired at $z\sim 1$ nm, and curves (III) and (IV) were acquired at $z\sim 0.8$ nm. (b) A random telegraph signal produced by sporadic tunneling of an electron back and forth between the probe and sample. The state in the sample is occupied for $\Delta f=0$ Hz and unoccupied for $\Delta f=2$ Hz. (c) Spectroscopy acquired at another site near 10-nm-thick SiO₂ showing that at some locations electrons may only tunnel either to or from a state and never return to their original configuration during the measurement. This may be caused by a post-tunneling energy relaxation process, or a movement of charge to nearby states inside the sample, but outside the tunneling range of the probe.

$z\sim 1$ nm and ramping the applied probe-sample dc voltage V while recording Δf . Figure 2(a) shows four such spectroscopic measurements at one location above a 10-nm-thick SiO₂ film. In each measurement, as the voltage is ramped downward, a state undergoes a transition from occupied to unoccupied near $V\sim -3.7$ V. As the voltage is ramped up, the state becomes occupied again in the same voltage range. The transition may occur abruptly, as a single step (I), or it may happen in a series of sporadic steps (II) as an electron tunnels back and forth between the probe and the state, producing a random telegraph signal (RTS). Similar RTSs, due to random occupation of charge traps in oxide layers, have been observed in the drain current of field-effect transistors and other devices.²¹ It is interesting to note that the RTS fluctuation rate is a few seconds, which appears to be set by the tunneling rate. If the probe-sample gap is reduced, the

RTS rate increases considerably, appearing as increased noise in the transition region as seen in Fig. 2(a) curves (III) and (IV). This effect is caused by the strong dependence of the tunneling rate on the probe-sample gap. Also, the voltage at which the transition occurs shifts to about -4.1 V because the fraction of the applied voltage dropped between the probe and the sample surface is decreased with the reduction in z . By fixing z and V to align the probe Fermi level with a state, RTS noise can be observed for up to 1 min or more. Figure 2(b) shows such a RTS measured at another location near a 10-nm-thick SiO_2 film with fixed $z \sim 1$ nm and $V = -5$ V. The state is occupied for $\Delta f = 0$ Hz and unoccupied for $\Delta f = 2$ Hz. The 2 Hz frequency shift associated with single-electron tunneling is greater than the frequency shift measured in Fig. 2(a) because the frequency shift depends upon both the applied voltage and the amplitude of probe oscillation, which are different for the two measurements.

The 1D electrostatic model places the energy level of the state observed in the measurements in Fig. 2(a) at 5.5 ± 0.2 eV below the SiO_2 conduction band edge. The uncertainty is due to the ± 0.3 nm uncertainty in the tunneling gap. The contact potential difference between the probe and sample is minimized prior to measurements by tuning the dc voltage to minimize the probe's frequency shift (flatband condition). The ~ 0.5 V width of the transition region corresponds to an ~ 0.15 eV uncertainty in the state energy. This transition energy width becomes smaller as the tunneling gap is reduced. The width of the Fermi distribution of the probe, the phonon broadening of the state, and the tunneling rate may all contribute to this transition width. The width of the transition is not fully understood and requires further study.

The results of spectroscopic measurements vary from place to place on the SiO_2 sample. At some locations, no tunneling is observed—indicating that no state is accessible by tunneling from the probe at that location. At other locations an electron tunnels in only one direction, and never returns, unless a large reverse bias is applied. Figure 2(c) shows two spectroscopy measurements near a 10-nm-thick SiO_2 film wherein an electron tunnels out of a state and does not return as the voltage ramp is reversed. This effect is likely caused by a post-tunneling change of the energy of the state (involving electron movement to or in nearby states) or

a lattice relaxation. Evidence for energy relaxation on the order of 1 eV in SiO_2 defects has been reported.²²

In summary, we have demonstrated a single-electron tunneling force spectroscopy method to directly measure the energy of an individual electronic state in a completely non-conducting surface. We also report the observation of a random telegraph signal by single-electron tunneling force spectroscopy. This method opens for exploration a whole class of materials and nanometer scale structures not accessible to conventional I - V scanning tunneling spectroscopy.

The authors acknowledge funds provided by the Semiconductor Research Corporation.

¹C. J. Chen, *Introduction to Scanning Tunneling Microscopy* (Oxford University Press, New York, 1993).

²P. J. M. van Bentum, R. T. M. Smokers, and H. van Kempen, *Phys. Rev. Lett.* **60**, 2543 (1988).

³J. Repp, G. Meyer, F. E. Olsson, and M. Persson, *Science* **305**, 493 (2004).

⁴P. G. Piva, G. A. DiLabio, J. L. Pitters, J. Zikovsky, M. Rezeq, S. Dogel, W. A. Hofer, and R. A. Wolkow, *Nature (London)* **435**, 658 (2005).

⁵M. E. Welland and R. H. Koch, *Appl. Phys. Lett.* **48**, 724 (1986).

⁶M. Carfà, L. Lanzi, E. Pallicchi, and G. Aloisi, *Rev. Sci. Instrum.* **75**, 497 (2004).

⁷L. J. Klein and C. C. Williams, *Appl. Phys. Lett.* **79**, 1828 (2001).

⁸L. J. Klein and C. C. Williams, *Appl. Phys. Lett.* **81**, 4589 (2002).

⁹E. Bussmann, D. J. Kim, and C. C. Williams, *Appl. Phys. Lett.* **85**, 2538 (2004).

¹⁰E. Bussmann, N. Zheng, and C. C. Williams, *Appl. Phys. Lett.* **86**, 163109 (2005).

¹¹M. T. Woodsides and P. L. McEuen, *Science* **296**, 1098 (2002).

¹²R. Stomp, Y. Miyahara, S. Schaer, Q. Sun, H. Guo, P. Grutter, S. Studenikin, P. Poole, and A. Sachrajda, *Phys. Rev. Lett.* **94**, 056802 (2005).

¹³A. Dana and Y. Yamamoto, *Nanotechnology* **16**, S125 (2005).

¹⁴J. Zhu, M. Brink, and P. L. McEuen, *Appl. Phys. Lett.* **87**, 242102 (2005).

¹⁵Y. Suganuma, P.-E. Trudeau, and A.-A. Dhirani, *Phys. Rev. B* **66**, 241405(R) (2002).

¹⁶Y. Azuma, M. Kanchara, T. Teranishi, and Y. Majima, *Phys. Rev. Lett.* **96**, 016108 (2006).

¹⁷Mikromaschi, NSC15 Ti-Pt.

¹⁸S. M. Sze, *Physics of Semiconductor Devices*, 2nd ed. (Wiley, New York, 1981).

¹⁹M. P. Seah and S. J. Spencer, *J. Vac. Sci. Technol. A* **21**, 345 (2003).

²⁰N. Zheng, C. C. Williams, and E. Mischenko (unpublished).

²¹K. S. Ralls, W. J. Skocpol, L. D. Jackel, R. E. Howard, L. A. Fetter, R. W. Epworth, and D. M. Tennant, *Phys. Rev. Lett.* **52**, 228 (1984).

²²T. Bakos, S. N. Rashkeev, and S. T. Pantelides, *Phys. Rev. Lett.* **91**, 226402 (2003).

Applied Physics Letters is copyrighted by the American Institute of Physics (AIP). Redistribution of journal material is subject to the AIP online journal license and/or AIP copyright. For more information, see <http://ojps.aip.org/aplo/aplcr.jsp>